AIAA JOURNAL
Vol. 33, No. 11, November 1995

Error Estimator and Adaptive Moving Grids for Finite Volumes Schemes

A. Ilinca,* R. Camarero,† J. Y. Trépanier,† and M. Reggio‡
École Polytechnique de Montréal, CERCA, Montréal, Québec H3C 3A7, Canada

A new adaptation technique has been developed for two- and three-dimensional grids, based on relocation of the mesh nodes. The flow is governed by the Euler equations expressed in an Euler–Lagrange form and the discretization uses a first-order finite volume scheme based on Roe's approximate Riemann solver. The grid is unstructured, and its motion and evolution obey the physical and geometrical conservation laws. The error is evaluated by a reconstructed, higher order solution, which is used to derive a forcing term to drive the motion of the grid nodes. This is formulated so as to uniformly distribute the error, while keeping the same grid connectivity. The development is made for two- and three-dimensional grids, although results are presented only for two-dimensional flows.

Introduction

THE adaptation of the grid to the flow characteristics is widely recognized as a method to improve the solution accuracy and the overall computing efficiency of numerical schemes. The motivation is that since the grid is normally generated before knowing the flow behavior, it is possible that the nodes distribution does not correspond to the solution requirements.

The adaptivity process is made up of two key elements: an error estimator and an adaptation procedure. The simplest error estimator, used for finite volume schemes,[1,2] is based on the physical behavior of the flowfield, more specifically on the gradient of the density or the Mach number. The adaptation consists in refining and coarsening the mesh in regions of higher or lower gradients respectively.

The projection method developed by Zienkiewicz and Zhu[3,4] is based on the observation that for finite elements discretization, the solution is continuous, whereas the derivatives are discontinuous at the interface of two elements. Those derivatives are projected in a space of continuous functions and the norm of the difference between this projection and the derivatives is used as a measure of the computational error. For some problems, the fluxes, instead of derivatives, are physically continuous in all of the domain and, consequently, more appropriate to be projected in a space of continuous functions.[5]

Babuska and Rheinboldt[6] propose an error estimator based on the solution of a local variational problem, where the unknowns are the approximation errors. The advantage consists in the reduction of the size of the linear system to be solved.

In compressible flows, with shock waves or contact discontinuities, the variables can no longer be considered continuous. The computed errors based on the solution gradient increase unboundedly with the adaptation of the discontinuity. This acts as permanent source for grid refinement and could produce wrong results.[7]

Paillére et al.[8] use a wave model to evaluate the error for compressible flows. The model combines the effects of the divergence and rotational of the velocity. To reduce the influence of discontinuities, the error is multiplied by a power of a characteristic length of the grid cell. The adaptation procedure also considers a minimal local grid size.

Received Dec. 16, 1994; presented as Paper 95-0669 at the AIAA 33rd Aerospace Sciences Meeting, Reno, NV, Jan. 9–12, 1995; revision received May 5, 1995; accepted for publication May 5, 1995.

*Ph.D. Student, Department of Mechanical Engineering, C. P. 6079, Succ. Centre Ville; currently Professor, Université du Québec à Rimouski, 300 allée des Ursulines, Rimouski, Québec G5L 3A1, Canada. Member AIAA.

†Professor, Department of Mechanical Engineering, C.P. 6079, Succ. Centre Ville. Member AIAA.

‡Professor, Department of Mechanical Engineering, C.P. 6079, Succ. Centre Ville.

Recently, Pelletier et al.[9] proposed an error estimator for hyperbolic problems, which rigorously takes into account the presence of discontinuities in the flowfield. Combined with an adaptation strategy, this method reduces the size of the sides on the discontinuities, which is not always desirable.

In the second step of the adaption process, the computed error is used to modify the grid to obtain a uniform error distribution. This can be accomplished by total remeshing, local refinement and coarsening, or simply by repositioning the nodes.

The total remeshing procedure has been applied mainly for two-dimensional flows because of the considerable amount of time required for a three-dimensional grid generation. Initially introduced by Zienkiewicz and Zhu,[3,4] the technique has been used for incompressible viscous flows[10,11] and for compressible flows.[12] To reduce significantly the computing time, local refinement and coarsening techniques have been considered as alternatives for two-dimensional[8,13] and three-dimensional[14,15] flows.

The adaptive strategies based on nodes displacement become particularly interesting for three-dimensional computations, where, because of memory limitation, the grid refinement is costly. Furthermore the grid management difficulties associated with refinement are avoided. Even if node redistribution, with a fixed connectivity, has limited degrees of freedom, some encouraging results have been obtained with such methods.

Nakahashi and Deiwert[16] consider an analogy with the elastic behavior of tension and torsion springs to redistribute the grid points. The mesh sides are replaced by springs with the stiffness related to the flow gradients and the nodes are moved until the spring system is in equilibrium. This analogy has been extended to three-dimensional flows by Davies and Venkatepathy.[17] However, the technique is still limited to structured meshes.

A common requirement to all of these adaptation procedures is an interpolation of the solution between two successive grids. For this reason the conservation laws are not rigorously respected and the errors could become important, especially for transient flows.

In this paper we propose an adaptive procedure applicable to unstructured meshes that is coupled with a first-order finite volume discretization of the Euler equations. The error estimator takes into account the flow behavior given by the density gradient and the local element size and orientation. It is based on the difference between the piecewise constant computed density and a reconstructed piecewise linear solution that conserves the mass.

The adaptation technique consists in moving the grid nodes by a velocity field related to the error distribution. For each node a velocity is computed in such a way that the point will move towards regions of higher error.[18] The Euler–Lagrange form of the flow equations expressed in conservative form allows a rigorously correct discretization of physical conservation laws. Furthermore, the movement of the grid nodes is such to ensure a perfectly conservative algorithm for geometry. The unstructured grid conserves its

connectivity and the flow variables are "transported" by the mesh elements.

Flow Solver and Geometric Conservation Laws

Using an arbitrary Euler–Lagrange formulation, the dimensionless Euler equations in the conservative form can be expressed as

$$\frac{\partial}{\partial t}\int_{V(t)} U\,\mathrm{d}V + \int_{S(t)} \boldsymbol{n}\cdot\mathcal{F}\,\mathrm{d}S = 0 \tag{1}$$

where $\boldsymbol{n}$ is the outward normal unit vector of the surface $S(t)$ enclosing the time-dependent volume $V(t)$ and $\boldsymbol{U}$ and $\mathcal{F}$ are defined by

$$\boldsymbol{U} = \begin{bmatrix} \rho \\ \rho\boldsymbol{u} \\ \rho E \end{bmatrix} \qquad \mathcal{F} = \begin{bmatrix} \rho\,(\boldsymbol{u}-\boldsymbol{\omega}) \\ \rho\boldsymbol{u}\,(\boldsymbol{u}-\boldsymbol{\omega}) + p\boldsymbol{I} \\ \rho E\,(\boldsymbol{u}-\boldsymbol{\omega}) + \boldsymbol{u}p \end{bmatrix} \tag{2}$$

where t is the time, ρ is the density, $\boldsymbol{u}$ is the flow velocity vector, $\boldsymbol{\omega}$ is the arbitrarily specified surface velocity, E is the total energy, p is the pressure, and $\boldsymbol{I}$ is the unit tensor. For static grids the velocity $\boldsymbol{\omega}$ simply reduces to zero in Eq. (2).

The conservative variables vector $\boldsymbol{U}$ is assumed constant over each cell, and the discretization of Eq. (1) is carried out according to an explicit first-order method.[19,20] The flux tensor $\mathcal{F}$ across the interface is computed using the Roe flux difference splitting (FDS) scheme.

For moving grids, in addition to the physical conservation laws, the so-called geometric conservation laws (GCL) must be carefully respected. These consist in two equations called, respectively, the surface conservation law (SCL) and the volume conservation law (VCL). The first law states that cell volumes must be bounded by its surfaces, whereas the second states that the volumetric increment of a moving cell must be equal to the sum of changes along the surfaces that enclose the volume. If these laws are violated, errors may be introduced in the flowfield in the form of sources and sinks of the conservative variables. The discretization of the geometric conservation laws follows the theory presented by Zhang et al.[21] and has been previously described and validated.[20]

Error Estimator

The role of the error estimator is to provide a measure of the grid quality, that is, the ability to correctly represent the flow characteristics and to provide information for the mesh adaptation.

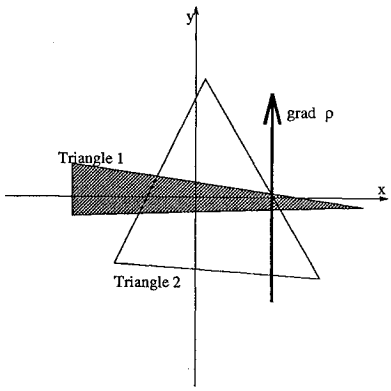

Fig. 1 Influence of the shape of the element on the error values.

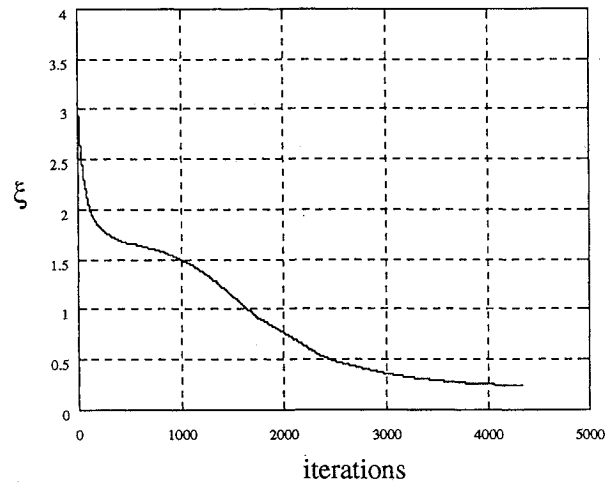

Fig. 3 Evolution of the error uniformity parameter in the adaptation process.

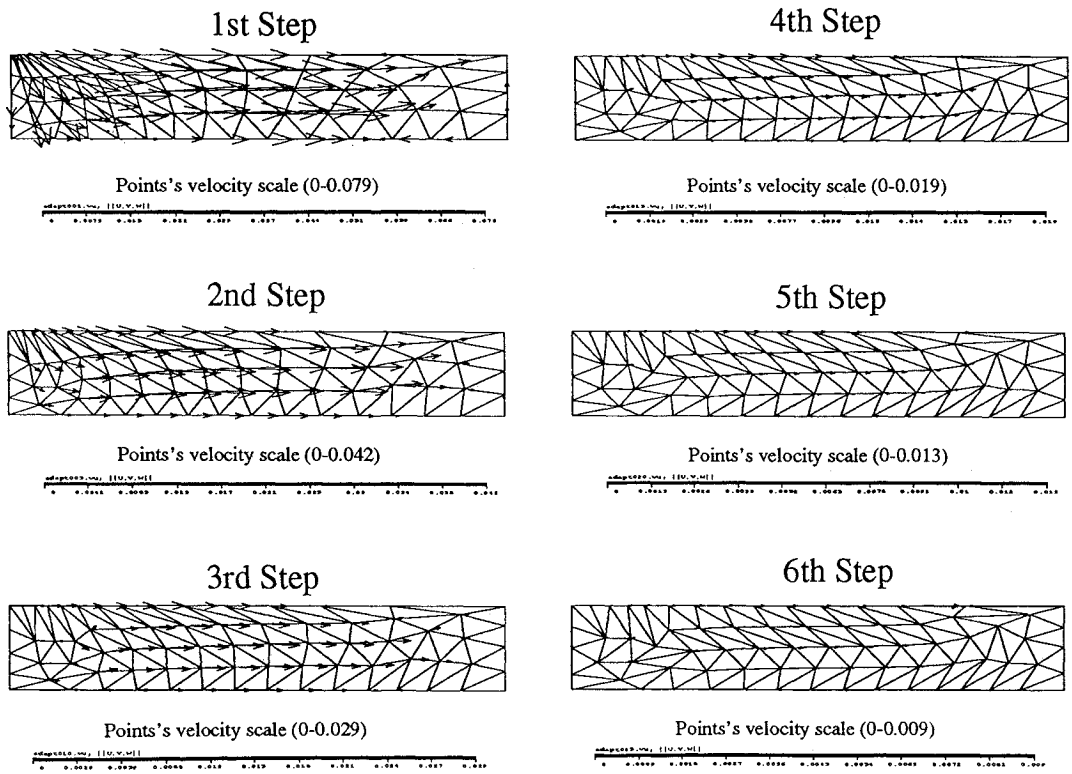

Fig. 2 Points velocities and mesh evolution to uniformly distribute the grid elements size.

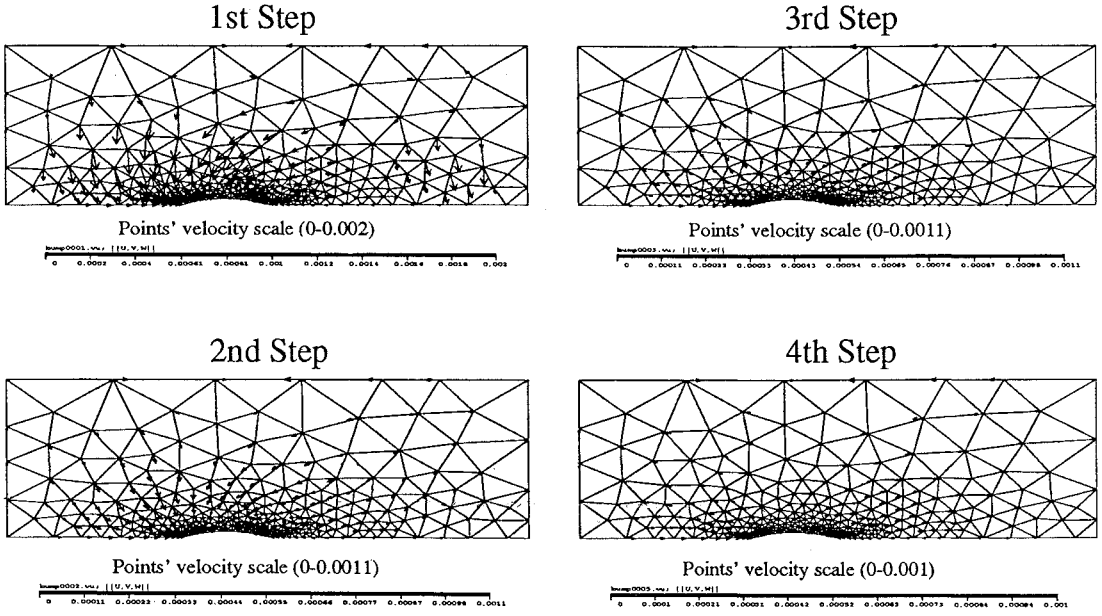

Fig. 4 Points velocities and mesh evolution for the subsonic flow over a bump.

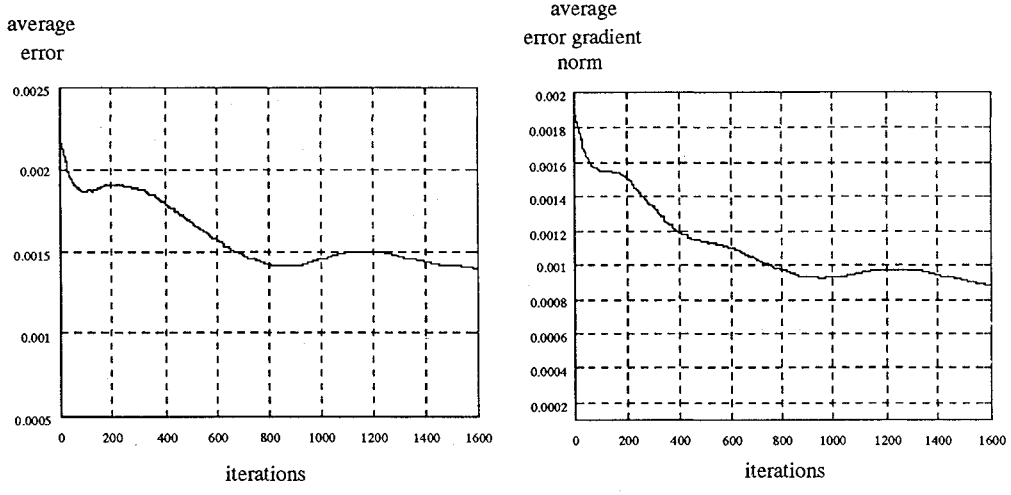

Fig. 5 Evolution of the average error and of the average norm of the error gradient.

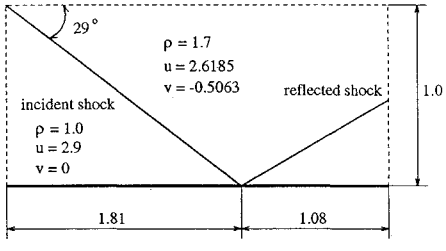

Fig. 6 Geometry and problem definition for the shock reflection.

An estimate is obtained by the difference between the computed solution, constant by element, and a reconstructed linear solution. The variable used for the analysis is the density, which is very representative of the flow behavior—stagnation zones, shock waves, and some contact discontinuities for compressible flows. Using a local Cartesian coordinate system defined with the origin at the center of the element, the linear solution on the element i has the form

$$\rho_i^1(x, y, z) = \rho_i^0 + \nabla \rho_i^1 \cdot \boldsymbol{r} \tag{3}$$

The superscript 0 represents the piecewise constant computed solution, whereas the superscript 1 denotes the reconstructed piecewise linear solution. The gradient is constant within each cell and the position vector $\boldsymbol{r}$ is given relative to the center of the element.

This reconstructed solution satisfies the mass conservation for each element i, of volume V_i, because

$$\int_{V_i} \left(\rho_i^1 - \rho_i^0\right) \mathrm{d}V = 0 \tag{4}$$

One method to evaluate the gradient that appears in Eq. (3) is to associate to each node k a density ρ_k^p given by the weighted average of its neighboring elements. The components of the gradient, for a triangular element, are then given by

$$\frac{\partial \rho^1}{\partial x} = \frac{\left(\rho_2^p - \rho_1^p\right)(y_3 - y_1) - \left(\rho_3^p - \rho_1^p\right)(y_2 - y_1)}{(x_2 - x_1)(y_3 - y_1) - (x_3 - x_1)(y_2 - y_1)}$$

$$\frac{\partial \rho^1}{\partial y} = -\frac{\left(\rho_2^p - \rho_1^p\right)(x_3 - x_1) - \left(\rho_3^p - \rho_1^p\right)(x_2 - x_1)}{(x_2 - x_1)(y_3 - y_1) - (x_3 - x_1)(y_2 - y_1)} \tag{5}$$

The error ε_i associated with the mesh element i is given by the norm of the difference between the computed and reconstructed solutions:

$$\varepsilon_i = \left\| \rho_i^1(x, y, z) - \rho_i^0 \right\| = \sqrt{\int_{V_i} \left[\rho_i^1(x, y, z) - \rho_i^0 \right]^2 \mathrm{d}V} \quad (6)$$

By replacing the expression (3) of the linear solution into Eq. (6), the error can be written in the form

$$\varepsilon_i = \sqrt{\int_{V_i} \left(\nabla \rho_i^1 \cdot \boldsymbol{r} \right)^2 \mathrm{d}V}$$

$$= \sqrt{\int_{V_i} \left(\left. \frac{\partial \rho^1}{\partial x} \right|_i x + \left. \frac{\partial \rho^1}{\partial y} \right|_i y + \left. \frac{\partial \rho^1}{\partial z} \right|_i z \right)^2 \mathrm{d}V} \quad (7)$$

As the integrals are computed in a reference frame with the origin at the center of the element, we obtain

$$\varepsilon_i = \left\{ \left(\left. \frac{\partial \rho^1}{\partial x} \right|_i \right)^2 I_x + \left(\left. \frac{\partial \rho^1}{\partial y} \right|_i \right)^2 I_y + \left(\left. \frac{\partial \rho^1}{\partial z} \right|_i \right)^2 I_z \right.$$
$$+ 2 \left. \frac{\partial \rho^1}{\partial x} \right|_i \left. \frac{\partial \rho^1}{\partial y} \right|_i I_{xy} + 2 \left. \frac{\partial \rho^1}{\partial y} \right|_i \left. \frac{\partial \rho^1}{\partial z} \right|_i I_{yz}$$
$$\left. + 2 \left. \frac{\partial \rho^1}{\partial z} \right|_i \left. \frac{\partial \rho^1}{\partial x} \right|_i I_{zx} \right\}^{\frac{1}{2}} \quad (8)$$

where the moments of inertia are defined by

$$I_x = \int_{V_i} x^2 \mathrm{d}V \qquad I_y = \int_{V_i} y^2 \mathrm{d}V \qquad I_z = \int_{V_i} z^2 \mathrm{d}V$$
$$I_{xy} = \int_{V_i} xy \, \mathrm{d}V \qquad I_{yz} = \int_{V_i} yz \, \mathrm{d}V \qquad I_{zx} = \int_{V_i} zx \, \mathrm{d}V \quad (9)$$

For two-dimensional situations the terms involving the z coordinate are not considered. The computation of those moments of inertia is common in mechanics of materials.

It is noted that this expression for the error accounts for the flow physics through the gradient components and the size and shape of the element through the moments of inertia. Figure 1 illustrates a situation when the density gradient is oriented in the y direction. From the computation point of view, the orientation of triangle 1 is preferable to that of the isotropic triangle 2. Because of the influence of the moments of inertia, the error for triangle 1 will be smaller than the error for triangle 2, even if the two elements have the same area. This particularity of the error estimator accounts for not only the size of the elements but also their orientation.

Adaptation Procedure

The mesh is adapted by applying a velocity to the grid points, whose value is related to the error distribution. This is analogous to the flow of a set of particles (i.e., the grid nodes) moving under the influence of a pressure gradient (i.e., the error gradient). This relationship is expressed by the following Poisson equation:

$$\nabla^2 \omega = -\nabla \varepsilon \quad (10)$$

Additional topological conditions are imposed to the mesh movement by assigning as boundary conditions that the nodes have the same velocity as the bounding surface on which they lie (i.e., Dirichlet type conditions) or can slide on that surface (Neumann type conditions). This will ensure that points initially on a boundary surface will remain on this surface, whereas the points initially inside the domain will not cross the boundary.

The adaptive procedure is related to the flow solver by introducing the ω velocity, the solution of Eq. (10), in the computation of flux tensor (2). The time step used for the grid displacement is the same as that for the flow solver, given by the Courant–Friedrichs–Lewy (CFL) criterion. The effect of the grid displacement will be to reduce the error gradient and, therefore, to uniformly distribute the error in the computational domain.

If the bounding surfaces of the domain are fixed (boundary points velocity is zero) and the error is uniformly distributed ($\nabla \varepsilon = 0$), the points velocities, as solution of Eq. (10), are zero. Therefore, theoretically, this adaptation procedure converges because the grid displacement stops when the error is uniformly distributed.

The discretization of Eq. (10) gives the velocity of point i as a linear combination of the error in the neighboring cells and velocities of the neighboring points[22]:

$$\omega_i = f(\varepsilon_{nb}, \omega_{nb}) \quad (11)$$

The objective of the grid adaptation is not to solve Eq. (10) until convergence but to establish the tendency of the grid points velocity. Therefore, in the adaptive procedure Eq. (11) is applied typically 20–50 times to all grid points, which is sufficient to diffuse the information concerning the error and, eventually, the motion of the boundaries. Also, a grid point's velocity is frozen for 20–100 iterations of the flow solver. This reduces the computer time for adaptation at about 1% of the global time. Furthermore, the use of Eq. (11)

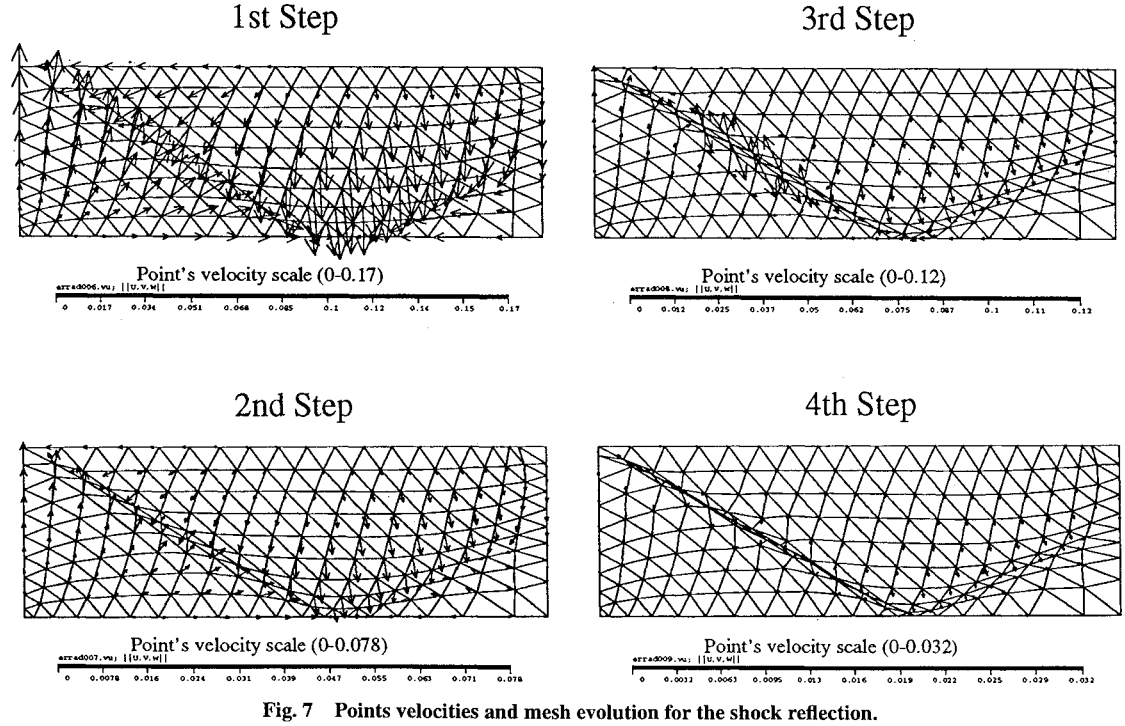

Fig. 7 Points velocities and mesh evolution for the shock reflection.

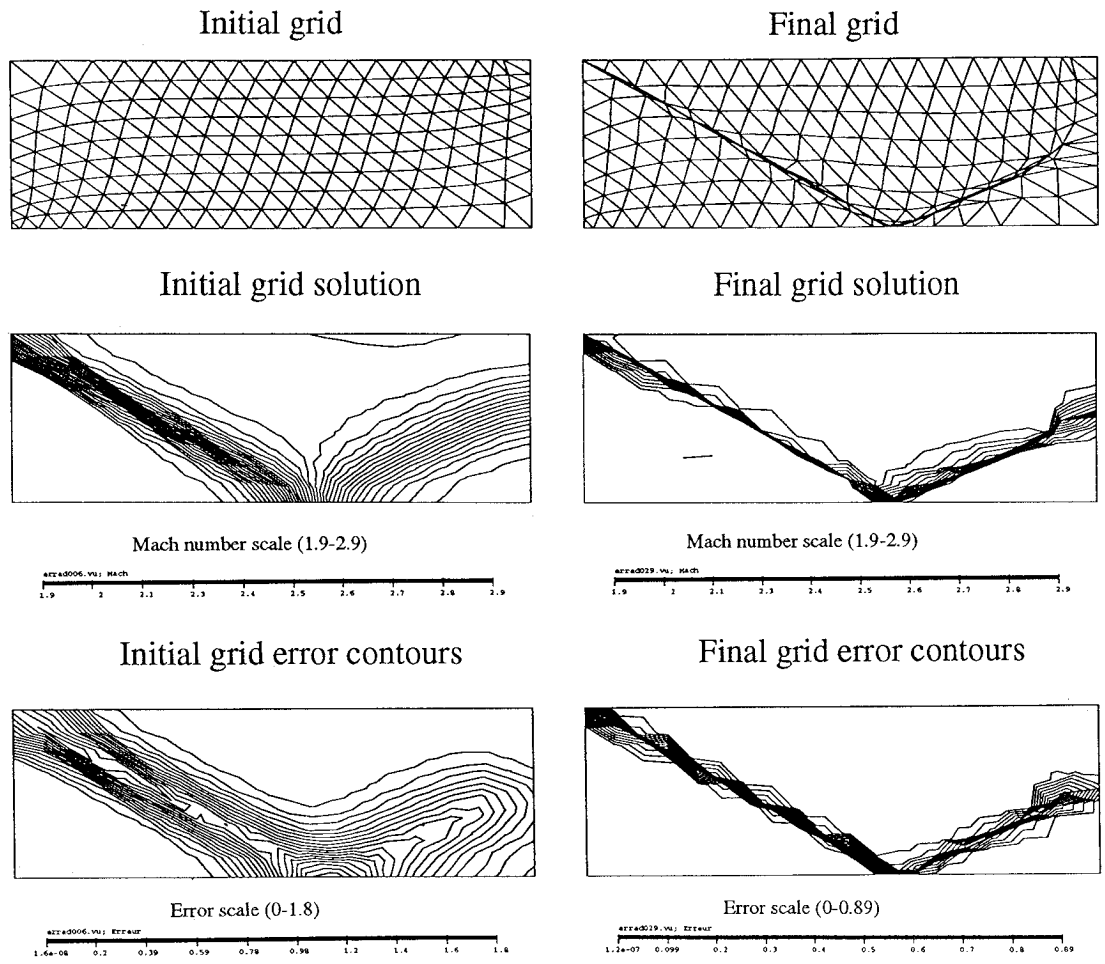

Fig. 8 Adaptation results for the coarse grid.

does not require additional storage as the grid points neighboring information is already present for the flow solver.

It is emphasized that, in the case of moving boundaries, the nodal velocity must be computed anyway and practically no overhead is introduced by the adaptation procedure. This is not the case with many existing adaptation techniques.

The described adaptation strategy becomes particularly useful if the initial number of grid elements approaches the limit allowed by the computer memory. This is the case for three-dimensional flows, where, to get the flow features properly, the initial grid should be very fine. In such conditions, the methods based on grid enrichment cannot be used and improvement of the solution can only be obtained by an appropriate redistribution of the existing points.

The most relevant advantage of this strategy is that the grid connectivity does not change and no interpolation is required. As point velocities instead of point positions are returned by the adaptation, the flow variables are transported with the mesh to the new location. The algorithm is ensured to be perfectly conservative by the proper discretization of the geometric conservation laws in the Euler–Lagrange formulation of governing equations.

Results

Adaptation Method Applied for Grid Size Uniformization

The first test is to verify that the velocity and displacement of the grid nodes can satisfy a specified adaptation criterion, where only the grid geometry is involved, that is, without introducing the flow characteristics. This is carried with a rectangular channel with an unstructured, highly nonuniform mesh containing 75 points and 112 elements. The supersonic flow in the channel is steady and uniform at Mach 1.5 and is not affected by external perturbations or by the grid velocity. The objective of the adaptation procedure is to obtain a uniform grid. Under such conditions the error associated with a

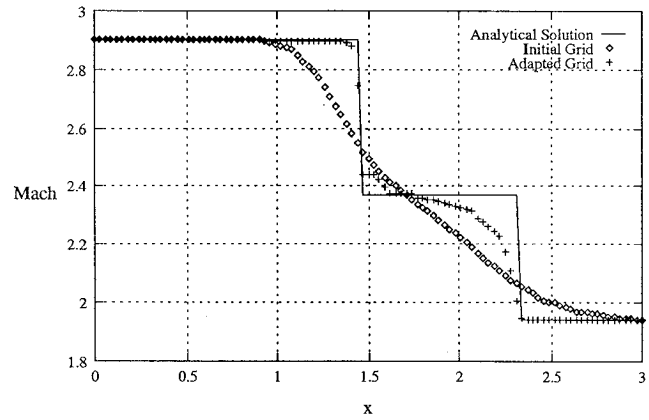

Fig. 9 Comparison of Mach number with analytic solution at a distance of $y = 0.2$ from the wall—solutions on the coarse grid.

grid element is given by the quotient between its volume V_i and the average volume of all elements (N is the total number of elements):

$$\varepsilon_i = \frac{V_i}{(1/N)\sum_{i=1}^{N} V_i} \tag{12}$$

The adaptation technique described previously, with the error given by relation (12), has to reduce the size of the triangles larger than the average and to increase those elements smaller than the average.

Figure 2 presents the evolution of the grid points velocity in the adaptation process. The velocities of the mesh points are larger at the beginning, which reflects the important differences in the mesh element size. The velocity of the points diminish as the grid tends to uniformity.

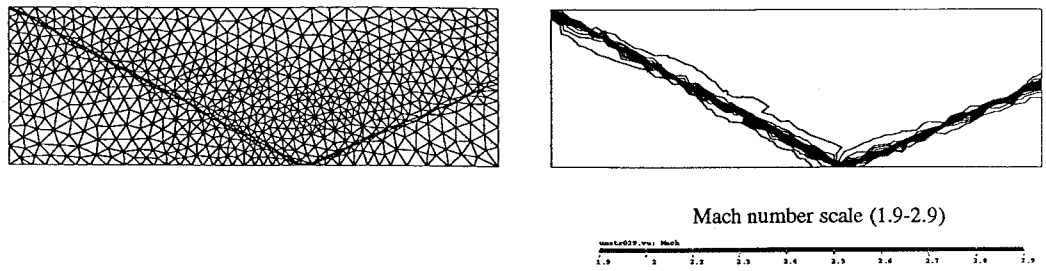

Fig. 10 Adaptation results on a fine grid.

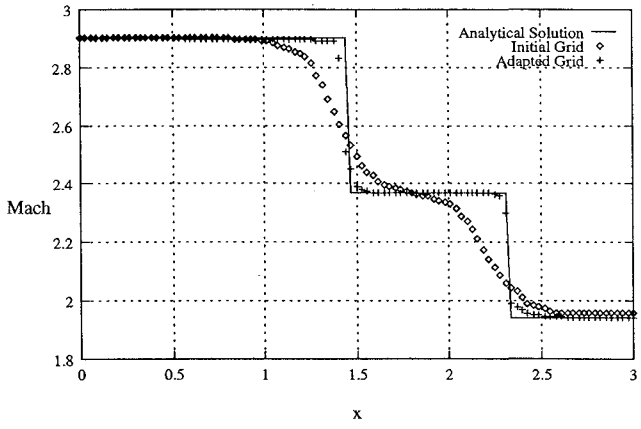

Fig. 11 Comparison of Mach number with analytic solution at a distance of $y = 0.2$ from the wall—solutions on the fine grid.

As a measure of the uniformity of the error, the parameter ξ, given by the difference between the maximal and minimal error, can be considered:

$$\xi = \varepsilon_{\max} - \varepsilon_{\min} = \frac{V_{\max} - V_{\min}}{(1/N)\sum_{i=1}^{N} V_i} \tag{13}$$

The evolution of this parameter in the adaptation process is shown in Fig. 3, where a reduction by a factor of 10 is obtained by moving the grid nodes. The large number of iterations is explained by the small time step for the grid displacement, identical to the one of the flow solver that has to satisfy the CFL criterion.

Subsonic Flow over a Bump

The second test consists in the subsonic flow over a bump, proposed by Parpia and Michalek.[23] The flow enters at $M = 0.6$ in the channel, and the circular arc has a 10% relative thickness. The initial grid is nonuniform and contains 304 nodes and 545 elements. Figure 4 illustrates the points velocities and the evolution of the grid in the adaptation process. The velocities diminish with the advancement of the solution from a maximum value of 0.002 at the beginning to 0.001 at the end of the adaptation process. This is due to the reduction of the error gradient.

A global measure of the adaptation technique is the average value of the error and of the error gradient norm. Their evolution in the adaptive process are shown in Fig. 5. We notice a 50% reduction of the average error obtained only by moving the grid points. In addition, a significant reduction of the error gradient has been obtained, which is the objective of the adaptation strategy and illustrates its effectiveness.

Shock Wave Reflection Problem

A more demanding test case is the reflection of a shock wave in a supersonic flow proposed by Peraire et al.[12] The geometry and the flow conditions are presented in Fig. 6. A very coarse mesh, containing 200 points and 342 triangles, is used to assess the capability of the method. The evolutions of the points velocities and of the mesh in the adaptation procedure are shown in Fig. 7. The initial mesh and the final adapted mesh are represented in Fig. 8. The high concentration and stretching of the grid in the shock region are noted.

The Mach number and the error contours are presented on the initial and on the final meshes in Fig. 8. On the adapted grid, in the neighborhood of the shocks, the triangles are very stretched and allow a sharp capture of the discontinuity. At Fig. 9 the variation of the Mach number at a distance of 0.2 from the bottom wall is compared with the analytic solution. On the initial grid the shocks are completely missed, and the Mach number is uniformly smeared across what should be the discontinuity. Meanwhile, as the adapted grid is also very coarse and a huge variation of element size and orientation occurs, the shock is not uniformly diffused on the mesh.

The element orientation plays an important role in the reduction of the error in the adaptation process. Unlike other error estimators,[8] the presence of the shock will not increase the error values once the grid is adapted. From Fig. 8 it is seen that the maximum error diminishes from 1.8 on the initial grid to 0.89 on the final one.

As the solver is first order accurate, at the exit of the channel a higher diffusion of the shock wave occurs, which negatively affects the grid quality in that region.

The procedure has also been applied for a mesh containing 816 points and 1541 triangles. The adapted mesh and the Mach number contours are presented in Fig. 10. This time, with a fine grid, the shock is better captured and symmetrically smeared. The comparison with the analytic solution at Fig. 11 enforces the solution improvement by using a finer mesh.

Grid Adaptation for the Transonic Flow over NACA 0012 Airfoil

The final test consists in the transonic flow over the NACA 0012 airfoil at a Mach number of 0.8 and 1.25-deg incidence. A strong shock occurs on the upper surface at about 60% of the chord length, whereas a weak shock appears on the lower surface at about 30% of the chord length.

The first grid used for computation is rather coarse and contains 3116 points and 6074 triangles. As the solver is first order accurate, the lower surface shock is not captured, whereas the shock on the upper surface is very sharp in the vicinity of the airfoil and is diffused as we move away in the flowfield. These characteristics are reflected by the error estimator and the adaptation procedure. In Fig. 12 the error distribution on the initial and adapted grid are composed. We notice the reduction from 0.62 to 0.38 in the maximum value of the error as well as the almost uniformly distributed error on the final grid.

Examination of the solution on the initial and adapted grids (Fig. 13) confirm the previous observations—good adaptation of the solution and sharp capture of the shock in the vicinity of the wall due to the nodes sliding on the surface, while far from the wall, the adaptation does not give the expected results and the shock is still diffused. The explanation is that the error estimator has been specifically developed for the first-order scheme. The solver's scheme is less accurate, which is more obvious when we compare the pressure coefficient distribution on the airfoil with the one of Cabello et al.,[24] obtained using a second-order finite volume Roe-based method on a grid containing 2711 points and 5300 triangles (see Fig. 14). Nevertheless, the adaptation procedure is able to adapt the grid where the discontinuities are detected by the solver.

Improvement of the solution quality is achieved by using a grid of 6479 nodes and 12781 triangles (Fig. 15). Although the solution

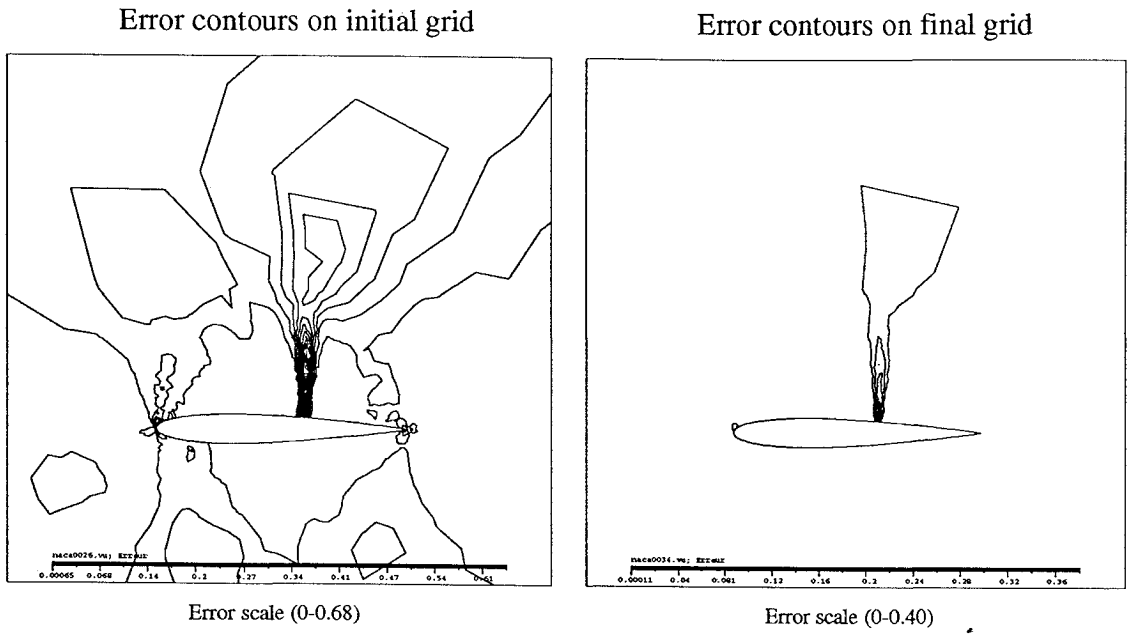

Fig. 12 Error contours on the initial and final grid for the flow over NACA 0012 airfoil (coarse grid solutions).

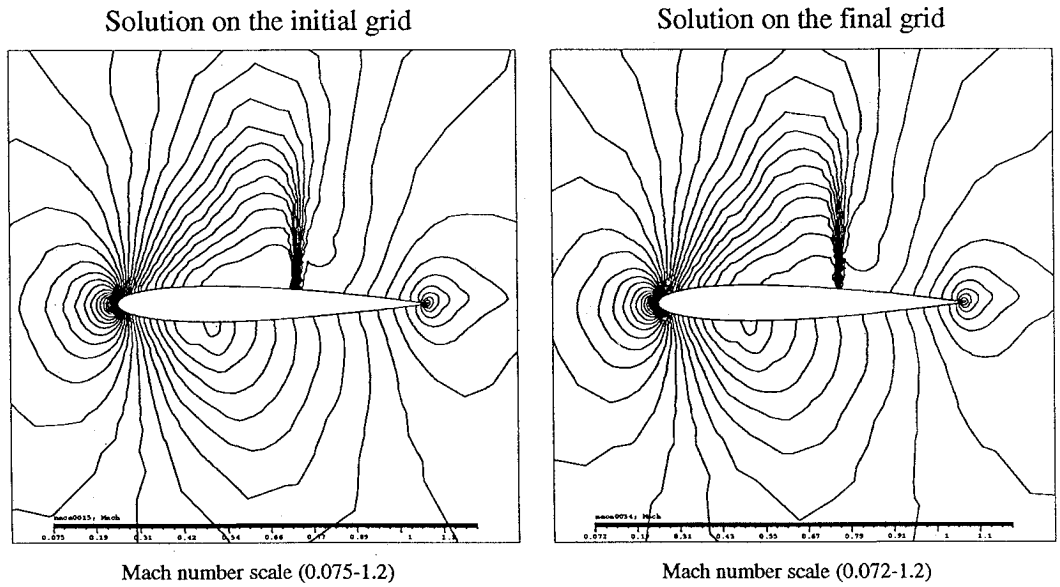

Fig. 13 Mach number contours on the initial and final grid for the flow over NACA 0012 airfoil (coarse grid solutions).

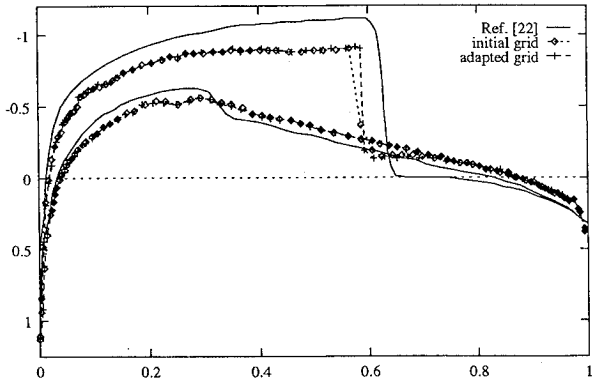

Fig. 14 Pressure coefficient on NACA 0012 airfoil with the initial and the adapted grid (computation on the coarse grid).

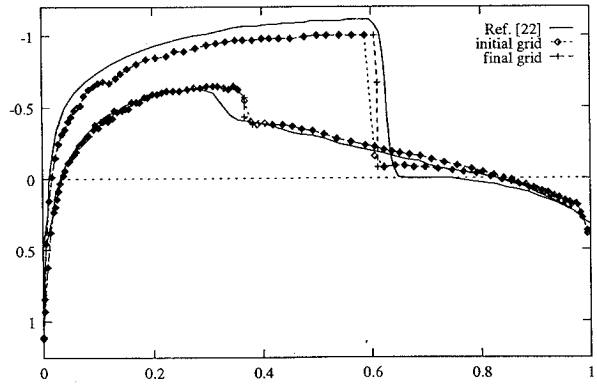

Fig. 15 Pressure coefficient on NACA 0012 airfoil with the initial and the adapted grid (computation on the fine grid).

approaches that of Cabello et al.[24] the initial grid contains a large number of points to capture the wake shock on the lower surface. In such conditions the solution improvement due to adaptation is less significant. The grid points move on the airfoil surface, and this leads to a very good capture of the shock on the upper surface, as can be seen in Fig. 14.

Conclusions

A new error estimation procedure and an adaptive method for unstructured grids has been proposed and developed. The error analysis is based on the reconstruction of a piecewise linear variation of density that is compared with the piecewise constant solution. The way this is done improves the existing methods by introducing the effect of the stretching and allowing a reduction in the error values during the adaptation process even in the vicinity of discontinuities. A possible improvement is to use the entire vector of conservative variables in the reconstruction process.

The adaptation technique is based on the redistribution of nodes by applying to them a velocity given by the error distribution. The intimate relation between the error and the grid evolution, as well as the way to rigorously satisfy the physical and geometrical conservation laws by eliminating the interpolation, are the principal assets of the proposed method. Theoretically the adaptation should drive to an optimal grid, on which the error is uniformly distributed. As mesh connectivity remains unchanged and consequently the degrees of freedom are limited, the uniformization of the error is possible only up to a certain point.

Encouraging results have been obtained using the method for subsonic, supersonic, and transonic flows. Further improvement is possible by changing the error estimator to work with more accurate discretization schemes.

References

[1]Reggio, M., Trépanier, J. Y., Zhang, H., and Camarero, R., "Numerical Simulation of the Gaz Flow in a Circuit Braker," *International Journal for Numerical Methods in Engineering*, Vol. 34, No. 4, 1992, pp. 607–618.

[2]Palmério, B., and Dervieux, A., "2D and 3D Unstructured Mesh Adaption Relying on Physical Analogy," *Proceedings of the Second International Conference on Numerical Grid Generation in CFD* (Barcelona), 1988, pp. 178–185.

[3]Zienkiewicz, O. C., and Zhu, J. Z., "A Simple Error Estimator and Adaptive Procedure for Practical Engineering Analysis," *International Journal for Numerical Methods in Engineering*, Vol. 24, No. 2, 1987, pp. 337–357.

[4]Zienkiewicz, O. C., and Zhu, J. Z., "Adaptivity and Mesh Generation," *International Journal for Numerical Methods in Engineering*, Vol. 32, No. 3, 1991, pp. 783–810.

[5]Ilinca, F., "Application d'une méthode d'éléments finis adaptative á des écoulements visqueux," M.S. Thesis, Ecole Polytechnique de Montréal, Montréal, Québec, Canada, 1993.

[6]Babuska, I., and Rheinboldt, W. C., "A Posteriori Error Estimator for the Finite Element Method," *International Journal for Numerical Methods in Engineering*, Vol. 12, No. 8, 1978, pp. 1597–1615.

[7]Warren, G., Anderson, W. K., Thomas, J., and Krist, S., "Grid Convergence for Adaptive Methods," *Proceedings of AIAA 10th Computational Fluid Dynamics Conference*, AIAA, Washington, DC, 1991, pp. 182–189.

[8]Paillére, H., Powell, K. G., and De Zeeuw, D., "A Wave Model Based Refinement Criterion for Adaptive Grid Computation of Compressible Flows," AIAA Paper 92-0322, 1992.

[9]Pelletier, D., Zaki, A., and Fortin, A., "Adaptive Remeshing for Hyperbolic Transport Problems," *International Journal for CFD* (to be published).

[10]Pelletier, D., and Hétu, J. F., "Adaptive Remeshing for Viscous Incompressible Flows," AIAA Paper 90-1604, 1990.

[11]Pelletier, D., and Hétu, J. F., "A Fast Adaptive Finite Element Scheme for Viscous Incompressible Flows," *Proceedings of AIAA 10th Computational Fluid Dynamic Conference*, AIAA, Washington, DC, 1991, pp. 139–150.

[12]Peraire, J., Vahdati, M., Morgan, K., and Zienkewicz, O. C., "Adaptive Remeshing for Compressible Flow Computations," *Journal of Computational Physics*, Vol. 72, No. 3, 1987, pp. 449–466.

[13]Trépanier, J. Y., and Yang, H., "ADX: Algorithms forAdaptive Discretisation based on Triangular Grids," École Polytechnique de Montréal, TR EPM/RT-93/3, Montréal Québec, Canada, 1993.

[14]Kallinderis, Y., Parthasarathy, V., and Wu, J., "A New Euler Scheme and Adaptive Refinement/Coarsening Algorithm for Tetrahedra Grids," AIAA Paper 92-0446, 1992.

[15]Biswas, R., and Strawn, R., "A New Procedure for Dynamic Adaption of Three Dimensional Unstructured Grids," AIAA Paper 93-0672, 1993.

[16]Nakahashi, K., and Deiwert, G. S., "Three Dimensional Adaptive Grid Method," *AIAA Journal*, Vol. 24, No. 6, 1986, pp. 948–954.

[17]Davies, C. B., and Venkatapathy, E., "Application of a Solution Adaptive Grid Scheme to Complex Three Dimensional Flows," *AIAA Journal*, Vol. 30, No. 10, 1992, pp. 2227–2233.

[18]Ilinca, A., Camarero, R., Trépanier, J. Y., Reggio, M., and Godin, J., "A NewAdaptive Technique Using Moving Grids," AIAA Paper 95-0669, 1995.

[19]Trépanier, J. Y., Reggio, M., Paraschivoiu, M., and Camarero, R., "Unsteady Euler Solutions for Arbitrarily Moving Bodies and Boundaries," AIAA Paper 92-0051, 1992.

[20]Ilinca, A., Trépanier, J. Y., Reggio, M., and Camarero, R., "Unsteady Three Dimensional Euler Solutions on Moving Grids," *Abstract of Papers Presented at the 4th CASI Aerodynamic Symposium* (Toronto), 1993, pp. 126–129.

[21]Zhang, H., Reggio, M., Trépanier, J. Y., and Camarero, R., "Discrete Form of GCL For Moving Meshes and Its Implementation in CFD Schemes," *Computers and Fluids Journal*, Vol. 22, No. 1, 1993, pp. 9–23.

[22]Ilinca, A., "Calcul des écoulements compressibles tridimensionnels sur des maillages en mouvement et adaptatifs," Ph.D.Thesis, École Polytechnique de Montréal, Montréal Québec, Canada, 1994.

[23]Parpia, I. H., and Michalek, D. J., "A Nearly Monotone Genuinely Multidimensional Scheme for the Euler Equations," AIAA Paper 92-0325, 1992.

[24]Cabello, J., Morgan, K., Lohner, R., Luo, H., and Baum, J., "An Implicit Solver for Laminar Compressible Flows on Unstructured Grids," AIAA Paper 95-0344, 1995.